Interhead tension determines processivity across diverse N-terminal kinesins

Shankar Shastry and William O. Hancock[1]

Department of Bioengineering, Pennsylvania State University, 205 Hallowell Building, University Park, PA 16802

Edited by Jonathan M. Scholey, University of California, Davis, CA, and accepted by the Editorial Board August 2, 2011 (received for review February 16, 2011)

Consistent with their diverse intracellular roles, the processivity of N-terminal kinesin motors varies considerably between different families. Kinetics experiments on isolated motor domains suggest that differences in processivity result from differences in the underlying biochemistry of the catalytic heads. However, the length of the flexible neck linker domain also varies from 14 to 18 residues between families. Because the neck linker acts as a mechanical element that transmits interhead tension, altering its mechanical properties is expected to affect both front and rear head gating, mechanisms that underlie processive walking. To test the hypothesis that processivity differences result from family-specific differences in neck linker mechanics, we systematically altered the neck linker length in kinesin-1, -2, -3, -5, and -7 motors and measured run length and velocity in a single-molecule fluorescence assay. Shortening the neck linkers of kinesin-3 (Unc104/KIF1A) and kinesin-5 (Eg5/KSP) to 14 residues enhanced processivity to match kinesin-1, which has a 14-residue neck linker. After substituting a single residue in the last alpha helix of the catalytic core, kinesin-7 (CENP-E) exhibited this same behavior. This convergence of processivity was observed even though motor speeds varied over a 25-fold range. These results suggest that differences in unloaded processivity between diverse kinesins is primarily due to differences in the lengths of their neck linker domains rather than specific tuning of rate constants in their ATP hydrolysis cycles.

cytoskeleton | molecular motor | intracellular transport | Monte Carlo model

N-terminal kinesins are involved in cellular tasks ranging from cargo transport to spindle organization and accordingly, the degree of processivity, defined as the number of steps a motor takes per interaction with a microtubule, varies from 1 to approximately 1,000 (1–4). Although positive charge in the neck-coil domain and the strength of dimerization have been proposed to play roles in processivity, differences in processivity between different N-terminal kinesin families are, like differences in motor speeds, generally thought to result from differences in the biochemical properties of their catalytic core domains (3, 5).

Processive motor stepping requires that the catalytic cycles of the two motor domains remain out of phase to avoid both heads being in a weak-binding or detached state. The inherent biochemical kinetics of each head domain play a role—for instance, a slow rate of hydrolysis or detachment from the microtubule should enhance processivity, whereas fast detachment in the ADP or ADP-P_i state should reduce processivity. However, the key mechanism for synchronizing the cycles of the two motor domains is intramolecular tension generated between the two head domains during phases of the cycle when both heads are bound to the microtubule. This coordination is described by two nonexclusive mechanisms: *front-head gating*—rearward tension on the front head prevents ATP binding until the trailing head detaches; and *rear-head gating*—binding of the leading head to the microtubule accelerates detachment of the rear head (6–8).

From stopped-flow experiments, it is clear that isolated motor domains from diverse kinesins possess widely varying catalytic rates for ATPase and microtubule detachment (5, 8, 9). However, the neck linker domain, which transmits intramolecular tension between the heads, also varies between kinesin families, ranging from 14 to 18 amino acids (10). The neck linker domain has three important roles in the kinesin chemomechanical cycle (Fig. 1). First, neck linker docking to the core motor domain is thought to be the key structural transition driving stepping. Second, binding of the free kinesin motor domain to the next binding site involves diffusion of the head, which is tethered by the entropic spring properties of the neck linker domain. Third, when both heads are simultaneously bound to the microtubule, the interhead mechanical forces that underlie coordination of their hydrolysis cycles are transmitted through the neck linker domains. The goal of the present work is to identify the degree to which the length of the neck linker controls motor properties for three diverse N-term kinesins: the axonal transport motor kinesin-3 (Unc104/KIF1A), the mitotic spindle motor kinesin-5 (KSP/Eg5), and the kinetochore motor kinesin-7 (CENP-E). This work builds on previous experiments on the transport motors kinesin-1 (conventional kinesin) and kinesin-2 (KIF3A/B) (11).

Kinesin-3 motors transport synaptic vesicles along axons, and mutations in kinesin-3 result in fewer synaptic vesicles in growth cones and early death (12). KIF1A monomers were shown to

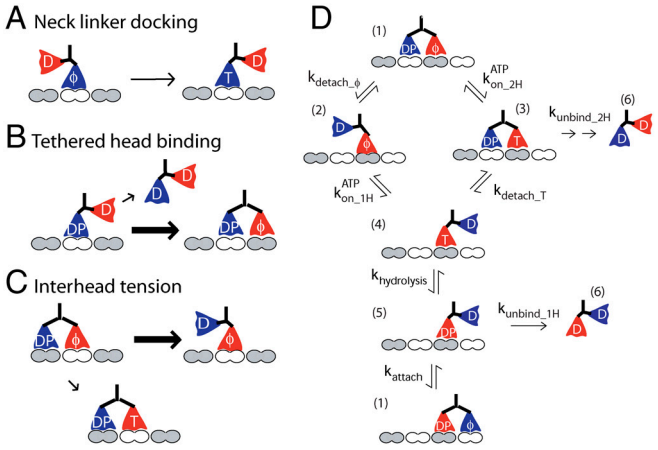

Fig. 1. Roles of the kinesin neck linker. In N-terminal kinesins, the neck linker plays three important roles. (*A*) Upon ATP binding, it docks to the catalytic core, producing a conformational change that positions the free head toward the next binding site. (*B*) During the diffusional search of the free head for the next binding site, the neck linker provides a tethering force, constraining the diffusional search. (*C*) When both heads are bound to the microtubule, tension between the two heads is transmitted through the neck linker domains and their shared coiled coil. (*D*) Model for the kinesin ATP hydrolysis cycle.

Author contributions: S.S. and W.O.H. designed research, performed research, analyzed data, and wrote the paper.

The authors declare no conflict of interest.

This article is a PNAS Direct Submission. J.M.S. is a guest editor invited by the Editorial Board.

[1]To whom correspondence should be addressed. E-mail: wohbio@engr.psu.edu.

This article contains supporting information online at www.pnas.org/lookup/suppl/doi:10.1073/pnas.1102628108/-/DCSupplemental.

move processively in vitro with mean run lengths of approximately 0.8 μm (13), facilitated through electrostatic interactions between the positively charged loop 12 (K loop) and the negatively charged C terminus of tubulin (14). Later work showed that kinesin-3 motors in vivo likely function as dimers, where dimerization is mediated either by cargo binding (15) or simply through stable dimerization of the motors (16).

Homotetrameric kinesin-5 motors (Eg5, KSP) (17) are required for proper organization of bipolar mitotic spindles during cell division (18), and small molecule inhibitors of Eg5 show promise as antimitotic drugs for cancer treatment (19, 20). Biochemical experiments on dimeric Eg5 suggest the motor is minimally processive (21, 22). In optical trapping experiments, Eg5 dimers on beads are minimally processive with mean run lengths of approximately 70 nm (3), though GFP-tagged Eg5 tetramers under no load move 0.6 μm per interaction, assisted by diffusional tethering of the motor to the microtubule (23). This moderate processivity is consistent with kinesin-5 motors working in groups to slide antiparallel overlapped microtubules, a function quite different from long-distance transporters such as kinesin-1.

The kinetochore-associated motor kinesin-7 (CENP-E) is required for proper alignment of chromosomes during metaphase (24, 25), and single-molecule experiments have demonstrated that CENP-E motors are processive kinesins that are capable of generating substantial forces (26–28). A kinetic analysis of CENP-E found that although the rate of neck linker docking in the monomer is relatively slow like Eg5, suggesting a less processive mechanism, the rear-head detachment rate in the dimer was only 1.5 times faster than the overall hydrolysis rate, suggesting the dimer spends most of its cycle in a two-head bound state, which should enhance processivity (5). Complicating these interpretations, half-site reactivity and turbidity experiments suggested that upon introduction of ATP many motors take one or only a few steps before dissociating, conflicting with the 250-step run lengths measured in single-molecule experiments.

Measured differences in the biochemical properties of isolated kinesin motor domains support the argument that variations in motor processivity result from differences in the properties of the catalytic core. A simple prediction is that engineered kinesin-3 motors should be highly processive due to their positively charged loop 12, kinesin-5 motors should be minimally processive due to their inherent biochemistry, and kinesin-7 engineered without the native neck-coil domain may be minimally processive due to removal of electrostatic tethering with the microtubule. On the other hand, we showed previously that processivity differences between kinesin-1 and kinesin-2 motors can be fully explained by differences in the lengths of their neck linker domains (11). This finding suggested that, although motor speed is determined by properties internal to the motor domain, processivity is controlled by mechanical communication between the motor heads, transmitted through the neck linker domains.

In the present work, we ask, *Does the length of the neck linker domain control processivity across diverse N-terminal kinesin families?* Although kinesin-1 has a 14 amino acid neck linker, kinesin-2 and kinesin-3 have 17 residue neck linkers, and kinesin-5 and kinesin-7 motors have 18 residue neck linker domains (10). In the literature there is significant dispersion in reported run lengths due to different buffer conditions and experimental techniques, but kinesin-3 and kinesin-7 motors have similar processivity as kinesin-1, kinesin-5 motors are minimally processive, and kinesin-2 motors are somewhere in between. If altering the neck linker domain results in similar changes in processivity across diverse kinesins, this argues that intramolecular strain between the two motor domains is the key determinant of processivity as opposed to the biochemical properties of the core motor domain.

Our approach was to fuse the head and neck linker domains of kinesin-3, -5 and -7 to the neck-coil and proximal coiled-coil region of kinesin-1 (Fig. 2) and measure motor run lengths and speeds in a single-molecule total internal reflection fluorescence (TIRF) assay. Dimerizing every motor using an identical neck-coil domain avoids any uncertainty due to unwinding of the coiled coil during stepping. Further, using a standard neck-coil domain and carrying out all experiments in 80 mM piperazine-*N*-*N*′-*bis*(2-ethanesulfonic acid) (Pipes) buffer minimize any influence of nonspecific electrostatic interactions on processivity. In earlier work Yildiz et al. found that large neck linker inserts had only a minimal effect on kinesin processivity, but we showed previously that processivity differences in that study were masked by a combination of positive charges introduced in the inserts and the use of low ionic strength buffers (11, 29). To test the influence of neck linker mechanics on kinesin stepping, the neck linker domain of each motor was systematically altered and the motor speed and processivity compared.

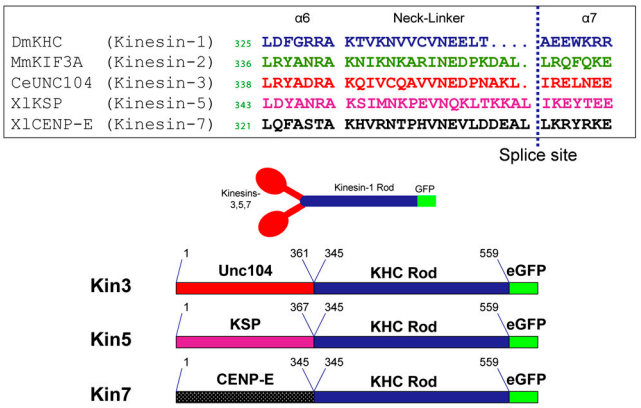

Fig. 2. Design of N-term kinesin constructs. Amino acid sequences of Kinesin-1, -2, -3, -5, and -7 motors with adjacent α-6 (catalytic core) and α-7 (neck coil) sequences. The catalytic core and neck linker of CeUnc104, XlKSP and XlCENP-E were fused to the neck coil and rod of DmKHC to make Kin3, Kin5, and Kin7, respectively.

Results and Discussion

Kinesin-3 Processivity Scales Inversely with Neck Linker Length. When the Unc104 head and 17-residue neck linker were fused to the kinesin-1 coiled coil and GFP, the resulting $Kin3_{17}$ construct moved processively with a mean run length of 0.62 ± 0.03 μm (mean ± SE of fit) and a speed of 2.77 ± 0.52 μm/s (mean ± SD) (Fig. 3*A*). This run length is somewhat less than the 1.5 μm measured for Unc104 dimerized by a Leu zipper downstream of its coiled-coil domain (30) and the 1.2 μm measured for a naturally dimeric KIF1A (16), but both of those measurements were performed in low ionic strength buffers, which enhance electrostatic interactions with the microtubule. In 12 mM Pipes buffer, $Kin3_{17}$ had a run length of 2.7 ± 0.2 μm, in reasonable agreement with these previous results.

When the neck linker of kinesin-3 was shortened to 14 amino acids ($Kin3_{14}$) to match the kinesin-1 neck linker length, the run length increased threefold to 1.87 ± 0.09 μm (mean ± SE of fit) (Fig. 3*B*), very similar to the kinesin-1 run length of 2.1 μm measured previously (11). This result is consistent with a highly processive dimer created previously by Tomishige et al., which consisted of the head and first 12 neck linker residues of Unc104 fused to the last two neck linker residues and coiled coil of kinesin-1 (30). To test the hypothesis that motor processivity scales with neck linker length, we made an intermediate construct, $Kin3_{15}$, whose run length was measured to be 0.95 ± 0.03 μm. Hence, like kinesin-1, processivity of kinesin-3 motors scales inversely with the length of their neck linker domain.

Kinesin-5 Processivity. To systematically characterize the influence of neck linker length on kinesin-5 motor processivity, the core

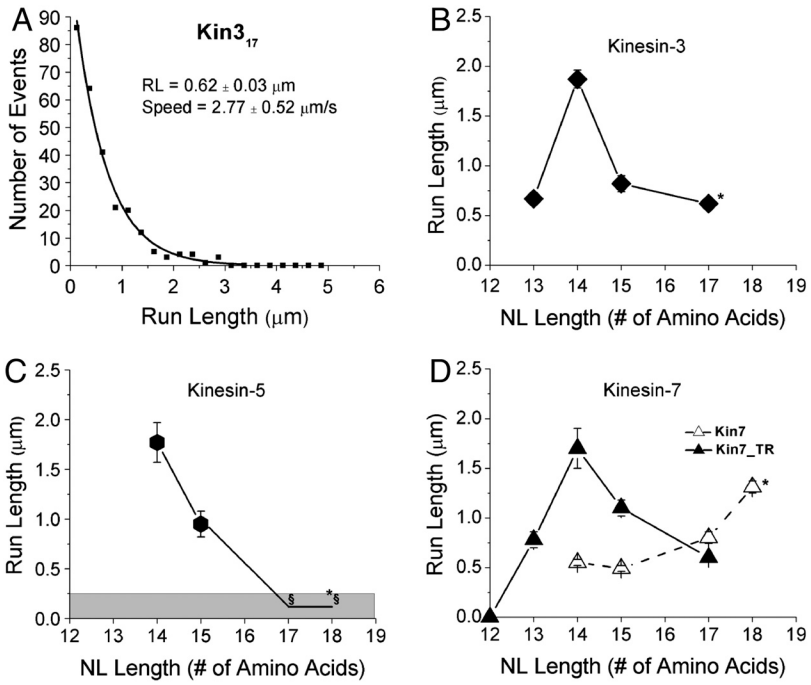

Fig. 3. Processivity scales with neck linker length. (*A*) Histogram of single-molecule runs of Kin3$_{14}$ from TIRF assay. The mean run length was calculated from a single exponential fit. (*B*) Run lengths of Kin3 constructs as a function of their neck linker (NL) length. Error bars represent the standard error from exponential fits and the asterisk denotes putatitve wild-type neck linker length. (*C*) Run lengths of different Kin5 constructs as a function of their neck linker length. Run lengths below 250 nm could not be reliably detected by our TIRF system and hence run lengths for Kin5$_{17}$ and Kin5$_{18}$ are estimates (upper limit of 250 nm) and shown in gray. (*D*) Run lengths of Kin7 constructs as a function of neck linker length. Kin7$_{TR}$ constructs have Thr$_{333}$ mutated to Arg as described in the text.

motor domain and neck linker of XlKSP were fused to DmKHC coiled coil and GFP (Kin5$_{18}$), and the neck linker length was varied from 18 to 14 amino acids. No single-motor runs were observed for Kin5$_{18}$ or Kin5$_{17}$ in 80 mM Pipes buffer, although the motors were active in a multimotor microtubule gliding assay (Table S1). As the lower limit of detection for processive events is approximately 250 nm, these results are consistent with processivity values for dimeric and tetrameric kinesin-5 reported previously (3, 23). In low ionic strength buffers, some processive runs were observed, but the high fluorescence intensity of the moving spots suggests these were motor aggregates and not single-molecule events.

When the neck linker domain was shortened to 14 residues by deleting the last four amino acids (ΔKKAL to make Kin5$_{14}$), processivity increased dramatically to 1.77 ± 0.20 μm (Fig. 3*C*), whereas the speed remained slow at 0.08 ± 0.02 μm/s (mean ± SD of mean). This result is similar to results from Lakamper et al. (31) who studied a similar construct. This result demonstrates that, to the degree that there are any unique kinetic characteristics of kinesin-5 that result in low processivity in the wild-type motor, they can be completely compensated for by shortening the neck linker to enhance head–head coordination. Lengthening the neck linker by one amino acid (Kin5$_{15}$) halved the run length to 0.95 ± 0.13 μm, in agreement with kinesin-1 containing a 15-residue neck linker (11), while having little influence on motor speed [0.09 ± 0.02 μm/s (mean ± SD)].

Kinesin-7 Processivity. In single-molecule fluorescence experiments, *Xenopus* CENP-E has been shown to be as processive as kinesin-1 and to generate comparable stall forces (27, 28). Disagreements in measured CENP-E motor speed and processivity have been explained by suggesting that the CENP-E coiled-coil region may possess a weak propensity for dimerization, may interact electrostatically with the microtubule to enhance processivity, or may sterically inhibit the motor domains in a phosphorylation-dependent manner (26–28, 32). Hence, fusing the *Xenopus* CENP-E head and neck linker domain to the stable and well-characterized kinesin-1 coiled coil is an ideal approach for clearly defining the motile properties of CENP-E.

From sequence analysis of the CENP-E neck region, the coiled coil either starts at Asp$_{342}$ or Leu$_{346}$, positions a and d of the heptad repeat. Because Asp never occupies the d position in kinesin neck coils or other well-characterized coiled coils, we conclude that CENP-E has an 18-residue neck linker domain (10, 33). When the entire 18-residue neck linker was included, these Kin7$_{18}$ motors had a run length of 1.31 ± 0.06 μm (mean ± SE of fit) and moved at a speed of 0.46 ± 0.07 μm/s. This run length is within 15% of the value measured by Kim et al. (27) in a comparable ionic strength buffer and it is half of that measured by Yardimci et al. (28) at low ionic strength (10 mM Pipes). We also made a similar construct using the head and neck linker of human CENP-E and found the motor moved at 10 nm/s, consistent with results from Gilbert lab (32). This result suggests that the slow speeds of human CENP-E are due to slow ATP hydrolysis or some other step in the hydrolysis cycle rather than misregistration of the coiled coil as has been suggested (5).

To test whether shortening the CENP-E neck linker enhances processivity, the run lengths of kinesin-7 motors with shorter neck linkers were characterized. Shortening the neck linker from 18 to 17 amino acids reduced the run length to 0.8 ± 0.06 μm (mean± SE of fit), and shortening it to 15 or 14 residues further reduced processivity to 0.49 ± 0.02 μm and 0.55 ± 0.02 μm, respectively (Fig. 3*D*). Motor speeds increased from 0.46 ± 0.07 μm/s for Kin7$_{18}$ to 0.57 ± 0.11 μm/s for Kin7$_{14}$ (Table S1). Hence, in contrast to the other N-terminal kinesins tested, kinesin-7 processivity decreased when its neck linker was shortened.

Alpha-6 Instability. In an effort to understand the divergent behavior of CENP-E, we analyzed family-specific sequences at the interface of the catalytic core and the neck linker. Our underlying hypothesis was that sequences that destabilize the end of helix α_6, thus extending the neck linker domain at its N-terminal end,

should have a similar effect as extending the neck linker at its C-terminal end, at least for states in which the neck linker is undocked. Notably, the neck linker is undocked in the free head as it undergoes tethered diffusion to its next binding site and in the leading head when both heads are bound to the microtubule (Fig. 1). The sequence RAK at the junction between the end of α-6 and the beginning of the neck linker is conserved across most N-terminal kinesin families, with a notable exception being kinesin-7, where both *Xenopus* and human CENP-E contain the sequence TAK (Fig. 2). If Thr_{333} in XlCENP-E destabilizes the end of α_6, this could lead to an effectively longer neck linker domain in kinesin-7. To test this prediction, Thr_{333} was mutated to Arg in $Kin7_{14}$, the motor for which tightening the neck linker should have the strongest effect on processivity. Although the speed of $Kin7_{14_{TR}}$ (0.55 ± 0.08 μm/s) was unaltered, the run length increased by a factor of three to 1.7 ± 0.24 μm, matching the processivity of other motors having 14 amino acid long neck linkers. Furthermore, the run lengths of $Kin7_{15_{TR}}$ and $Kin7_{17_{TR}}$ varied inversely with neck linker length, matching the results for kinesins-1, -2, -3, and -5 (Fig. 3*D*).

If Thr_{333} is indeed destabilizing the end of α_6 and functionally extending the kinesin-7 neck linker, then converting RAK in kinesin-1 to TAK would be predicted to reduce processivity in a similar manner. To test this prediction, Arg_{329} was mutated to Thr_{329} in Kin1 to create $Kin1_{RT}$. This motor was functional in a microtubule gliding assay with a velocity of 0.48 ± 0.02 μm/s, but no single-molecule runs were observed in the TIRF assay, suggesting the motor is nonprocessive. Extending the neck linker of $Kin1_{RT}$ to 17 residues did not rescue processivity, suggesting that the effect of the $T \rightarrow R$ substitution is not simply to shorten the neck linker. As this mutation is in the core motor domain, it is perhaps not surprising that it strongly alters motor behavior; one interpretation is that terminating α_6 with RAK represents an "optimal" structure and there are other compensating amino acid substitutions in Kin7 that are not present in Kin1.

Implications for the Kinesin Hydrolysis Cycle. Why does processivity depend so strongly on neck linker length? Below, we analyze the three potential mechanisms by which altering the neck linker may regulate processivity: neck linker docking, tethered diffusion, and transmission of interhead tension (Fig. 1).

Following ATP binding, the kinesin neck linker is thought to transition from an unstructured coil to a beta-strand conformation, which is stabilized by the N-terminal "cover bundle" (34–37). Stabilizing interactions between conserved residues in the neck linker and the core motor domain have been worked out from structural studies on kinesin-1 (34, 35, 38), and there is no evidence from existing crystal structures of other motors having longer neck linkers that residues beyond the 14 present in kinesin-1 participate in neck linker docking. This idea is supported by the fact that motor velocities of kinesin-2, -3, -5, and -7 are not substantially altered by deleting residues beyond the 14 present in kinesin-1. Hence, we discount the hypothesis that altering the neck linker length at the C terminus controls processivity by altering docking to the catalytic domain.

The role of the neck linker domain in tethered diffusion of the free head was recently investigated by our group using Brownian dynamics simulations (39). If the neck linker is modeled as a worm-like chain, the neck linker is expected to strongly hinder the diffusion of the tethered head to the next binding site, and a large force between the heads (>30 pN) is expected in the two-head bound state. Extending the neck linker is expected to relieve this constraint and thus accelerate the rate that the tethered head binds to the next binding site. Because this one-head bound state (state 5 in Fig. 1*D*) is vulnerable to detachment, which will end a processive run, extending the neck linker domain is expected to, if anything, enhance processivity. Hence, we discount the hypothesis that altering the neck linker controls processivity by altering the tethered diffusion step in the hydrolysis cycle.

In contrast to these other mechanisms, extending the neck linker length *is* expected to reduce the mechanical coordination (or "gating") between the head domains. The "rear-head gating" model holds that detachment of the trailing head is slow until the lead head binds and exerts a force that accelerates its detachment, while the "front-head gating" model holds that rearward tension in the two-head bound state prevents ATP binding until the trailing head detaches (Fig. 1*C*). Both mechanisms work to maximize the number of steps the motor takes before detachment, and each involves interhead tension transmitted via their neck linkers and shared coiled coil. Thus for both gating mechanisms, extending the neck linker domain is expected to decrease the tension between the motor domains and thereby decrease processivity.

Using a Monte Carlo modeling approach and parameter sets (Table S2) developed previously (11, 40), we tested whether the experimental results could be explained by an effect of neck linker length on front- or rear-head gating. The neck linker was modeled as a worm-like chain and interhead tension in the two-head bound state calculated as the force required to stretch each neck linker by 4 nm. Front-head gating was modeled by incorporating a force-dependent $k_{on_{ATP}2H}$ such that longer neck linkers led to faster ATP binding rates (see Fig. 1*D*). Rear-head gating was modeled by making k_{detach} force dependent such that longer neck linkers reduced the detachment rate. As seen in Fig. 4*C*, both mechanisms were able to account for the steep dependence of run length on neck linker length. Furthermore, both gating mechanisms were consistent with neck linker length having only a minor effect on velocity (Fig. 4*D*). Thus, the results can be quantitatively accounted for by neck linker extension diminishing either front- or rear-head gating. In both scenarios, extending the neck linker increases the probability of state 3 (Fig. 1*D*) being occupied, which leads to premature dissociation of the motor from the microtubule.

Implications for Diverse N-Terminal Kinesins. The most significant finding from this study is that when the neck linkers are shortened to 14 residues and fused to the kinesin-1 coiled coil, kinesin-3, kinesin-5, and kinesin-7 (following Thr → Arg substitution in alpha-6) quantitatively match the processivity of the canonical kinesin-1. This result suggests that differences in unloaded processivity between diverse kinesins is primarily due to differences in the lengths of their neck linker domains (which presumably controls interhead tension) rather than specific tuning of rate constants in their ATP hydrolysis cycles. Although differences in kinetic rates clearly lead to different motor speeds and may result in different responses to external loads, the present results impact a number of studies in the literature and provide an important constraint for ongoing studies of diverse kinesins.

One unique feature of kinesin-3 motors is a positively charged insert (the K loop) into the microtubule-binding loop 12 of the motor domain, which may be expected to enhance the processivity of Unc104 dimers (13). However, when the Unc104 head and its entire 17-residue neck linker were fused to the kinesin-1 neck coil, the run length was 0.6 μm in 80 mM Pipes. Although this run length is 50% greater than kinesin-1 containing a neutral or negatively charged three-residue insert, it is only half that of a kinesin-1 containing a positively charged insert ($kinesin\text{-}1_{KAL}$), which matches the net charge of the last three residues (AKL) in the Unc104 neck linker (11). Furthermore, when the Unc104 neck linker was shortened to 14 residues, the run length was within 15% of kinesin-1. Hence, the K loop appears to play a minimal role in processivity of kinesin-3 dimers in moderate ionic strength buffers, contrary to expectations.

Although kinesin-5 containing its native neck linker was less processive than other motors with similar length neck linkers,

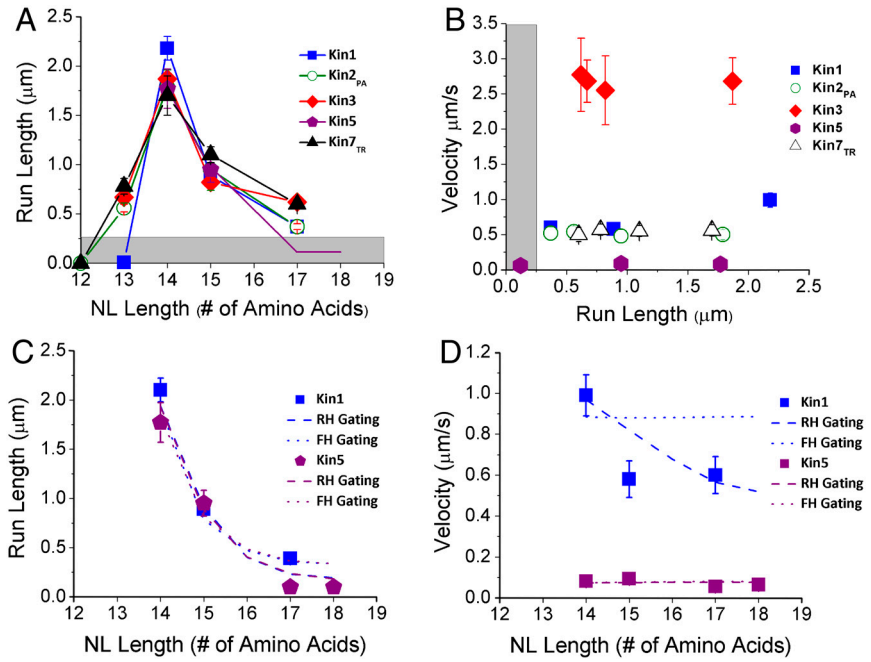

Fig. 4. Summary of run length and velocity data. (*A*) Results from Fig. 3 combined with results from Shastry (11), demonstrating that run lengths for diverse N-terminal motors scale inversely with neck linker length. (*B*) Motor velocity plotted as a function of run length for constructs having different neck linker lengths. Results show that, although changing neck linker length has dramatic effects on run length, it has a minimal influence on unloaded motor velocity. Run length and velocity results for all motors studied are presented in Table S1. (*C* and *D*) Kin1 and Kin5 simulation results using model shown in Fig. 1 and incorporating force-dependent rates for rear-head (RH) or front-head (FH) gating. Experimental results shown as solid points. Details of simulations and parameter sets used are given in *SI Text* and Table S2.

when the neck linker was shortened to 14 residues, kinesin-5 was just as processive as kinesin-1. It has been proposed that the minimal processivity of human Eg5 is due to some combination of slow docking of the neck linker to the core motor domain, slow or gated ATP binding to the head, and rapid dissociation of the head in the ADP state (5, 9). At a minimum, the robust processivity for $Kin5_{14}$ argues that shortening the neck linker to enhance head–head communication can completely override these properties of the core motor domain.

The outlier in the kinesin motor families tested in this work is kinesin-7. Both *Xenopus* and human CENP-E have been shown to be processive in vitro, but there has been some debate as to precisely how processive the wild-type motor is and what role the coiled-coil domains play in electrostatic tethering, dimerization, and motor regulation (27, 28, 32). In our hands, dimeric wild-type *Xenopus* CENP-E containing a wild-type neck linker is more processive than other motors with similar length neck linkers, but it is less processive than wild-type kinesin-1. As the kinesin-7 neck linker (particularly the distal portion) has a net negative charge, and because kinesin-7 motors do not contain a K loop, this result cannot be explained by electrostatic tethering to the microtubule by the head or neck linker domains. A recent comparison of the kinetic properties of monomeric CENP-E and KHC found that although some characteristics, such as slow dissociation in the ADP state, may provide an explanation for enhanced processivity of CENP-E, other characteristics such as the 10-fold slower neck linker docking rate suggests that CENP-E should be minimally processive like Eg5 (5); hence, there is no clear indication from CENP-E kinetics that it should be more processive than an analogous kinesin-1 construct. Further, it is not clear from structural or kinetic data why shortening the kinesin-7 neck linker should not enhance processivity as it did for all other motors tested.

We found that changing one residue at the head:neck interface reduced processivity of kinesin-7 with a wild-type neck linker but enhanced processivity of constructs with shorter neck linker domains. The hypothesis motivating this mutation was that the divergent TAK sequence at the head:neck interface destabilizes the end of alpha-6, extending the neck linker at its proximal end. If this were the case, then we would expect that shortening the neck linker at its distal end should enhance processivity similar to the other families tested; hence, the explanation cannot be that simple. One possible interpretation is that the TAK sequence destabilizes the end of alpha-6 such that when the neck linker is shortened, resulting in higher interhead forces in the two-head bound state, the end of the helix unfolds. This would explain the lack of processivity enhancement upon shortening the neck linker, but it still does not explain the design advantage that leads to enhanced processivity of the 18-residue neck linker construct. The fact that introducing this TAK sequence into kinesin-1 destroys processivity highlights the importance of this "pivot point" in head–head coordination.

In our previous work (11), we examined the effect of altering the neck linker in kinesin-1 and kinesin-2, two motors that have similar transport roles in cells. The current study investigates N-terminal kinesins that have widely varying kinetic properties and divergent intracellular roles. Strikingly, these diverse motors show a similar dependence of unloaded processivity on neck linker length, suggesting processivity is controlled by a common mechanism. An important N-terminal kinesin family that this study does not address is kinesin-8 motors, which both move highly processively along microtubules and alter microtubule dynamics at microtubule plus-ends (4, 41). Although full-length motors are considerably more processive than kinesin-1 (4), in order to determine whether kinesin-8 motors present an exception to the present results, it will first be necessary to define the contribution of both the kinesin-8 tail domain and the expanded loop 2 to the observed kinesin-8 processivity.

Neck Linkers Shorter Than 14 Residues. We previously found that shortening the kinesin-1 neck linker from 14 to 13 residues abolished processivity, a result that suggested that neck linkers shorter than 14 residues are unable to extend the 8 nm required

for both heads to simultaneously bind to the microtubule (11). Surprisingly, when their neck linkers were shortened to 13 residues, $Kin2_{PA}$, Kin3, and $Kin7_{TR}$ were all processive, though their run lengths were significantly less than the corresponding motors with 14 residue neck linkers (Fig. 4*A*). Because of its positively charged K loop and the fact that monomers have been shown to be processive under certain conditions (13), this result can perhaps be understood for kinesin-3. However, understanding why the shortened kinesin-2 and kinesin-7 are processive and the kinesin-1 is not will require a more detailed kinetic analysis of these motors.

Conclusions. These experiments demonstrate that the length of the kinesin neck linker domain is the primary determinant of unloaded processivity across five different N-terminal kinesin families. This result suggests that the range of run lengths between these diverse motors results not from tuning of biochemical rate constants in their motor domains, but rather from differences in head–head communication due to their neck linker domains. Although the extent to which the motor properties diverge when the motor is moving against an external load is still being defined, these results demonstrate a striking commonality in mechanism across N-terminal kinesin families and provide important constraints for designing kinetics experiments to identify key rate constants that determine their diverse behavior.

Methods

Motor Constructs and Protein Expression. Kin1 was made by fusing *Drosophila* conventional kinesin truncated at position 559 to a C-terminus eGFP and His_6 tag, as previously described (11). To generate other Kin3, Kin5, and Kin7 constructs, the motor domains and associated neck linker sequences were amplified by PCR, digested with restriction enzymes, and ligated into the Kin1 plasmid, replacing the kinesin-1 head. Neck linkers were shortened and lengthened using the Stratagene Quick-change II XL site-directed mutagenesis kit, and all final constructs were confirmed by sequencing. All motors were expressed in bacteria and purified by Ni column chromatography as previously described (11).

Motility Assays. Bovine brain tubulin was purified, labeled with Cy5 (GE Healthcare), polymerized, and taxol-stabilized as previously described (11). Single-molecule TIRF experiments were performed at 26 °C, images were captured with a Cascade 512 CCD camera (Roper Scientific), and acquisition and image analysis were carried out using MetaVue software (Molecular Devices Corporation) with a 71-nm pixel size (11). To ensure that all events were reliably captured, only events with a minimum run length of 250 nm were analyzed, and this minimum distance was subtracted from all runs (this assumes detachment probability is independent of distance the motor has moved).

Computational modeling details are discussed in *SI Text*.

ACKNOWLEDGMENTS. This work was supported by National Institutes of Health Grant R01 GM076476 (to W.O.H.).

1. Block SM, Goldstein LS, Schnapp BJ (1990) Bead movement by single kinesin molecules studied with optical tweezers. *Nature* 348:348–352.
2. Howard J, Hudspeth AJ, Vale RD (1989) Movement of microtubules by single kinesin molecules. *Nature* 342:154–158.
3. Valentine MT, Fordyce PM, Krzysiak TC, Gilbert SP, Block SM (2006) Individual dimers of the mitotic kinesin motor Eg5 step processively and support substantial loads in vitro. *Nat Cell Biol* 8:470–476.
4. Varga V, et al. (2006) Yeast kinesin-8 depolymerizes microtubules in a length-dependent manner. *Nat Cell Biol* 8:957–962.
5. Rosenfeld SS, et al. (2009) The ATPase cycle of the mitotic motor CENP-E. *J Biol Chem* 284:32858–32868.
6. Block SM (2007) Kinesin motor mechanics: Binding, stepping, tracking, gating, and limping. *Biophys J* 92:2986–2995.
7. Hancock WO, Howard J (1999) Kinesin's processivity results from mechanical and chemical coordination between the ATP hydrolysis cycles of the two motor domains. *Proc Natl Acad Sci USA* 96:13147–13152.
8. Rosenfeld SS, Fordyce PM, Jefferson GM, King PH, Block SM (2003) Stepping and stretching. How kinesin uses internal strain to walk processively. *J Biol Chem* 278:18550–18556.
9. Rosenfeld SS, Xing J, Jefferson GM, King PH (2005) Docking and rolling, a model of how the mitotic motor Eg5 works. *J Biol Chem* 280:35684–35695.
10. Hariharan V, Hancock WO (2009) Insights into the mechanical properties of the kinesin neck linker domain from sequence analysis and molecular dynamics simulations. *Cell Mol Bioeng* 2:177–189.
11. Shastry S, Hancock WO (2010) Neck linker length determines the degree of processivity in Kinesin-1 and Kinesin-2 motors. *Curr Biol* 20:939–943.
12. Hirokawa N, Noda Y (2008) Intracellular transport and kinesin superfamily proteins, KIFs: Structure, function, and dynamics. *Physiol Rev* 88:1089–1118.
13. Okada Y, Hirokawa N (1999) A processive single-headed motor: Kinesin superfamily protein KIF1A. *Science* 283:1152–1157.
14. Okada Y, Hirokawa N (2000) Mechanism of the single-headed processivity: Diffusional anchoring between the K-loop of kinesin and the C terminus of tubulin. *Proc Natl Acad Sci USA* 97:640–645.
15. Klopfenstein DR, Tomishige M, Stuurman N, Vale RD (2002) Role of phosphatidylinositol(4,5)bisphosphate organization in membrane transport by the Unc104 kinesin motor. *Cell* 109:347–358.
16. Hammond JW, et al. (2009) Mammalian kinesin-3 motors are dimeric in vivo and move by processive motility upon release of autoinhibition. *PLoS Biol* 7:e72.
17. Kashina AS, et al. (1996) A bipolar kinesin. *Nature* 379:270–272.
18. Kashina AS, Rogers GC, Scholey JM (1997) The bimC family of kinesins: Essential bipolar mitotic motors driving centrosome separation. *Biochim Biophys Acta* 1357:257–271.
19. DeBonis S, et al. (2004) In vitro screening for inhibitors of the human mitotic kinesin Eg5 with antimitotic and antitumor activities. *Mol Cancer Ther* 3:1079–1090.
20. Mayer TU, et al. (1999) Small molecule inhibitor of mitotic spindle bipolarity identified in a phenotype-based screen. *Science* 286:971–974.
21. Crevel IM, Lockhart A, Cross RA (1997) Kinetic evidence for low chemical processivity in ncd and Eg5. *J Mol Biol* 273:160–170.
22. Lockhart A, Cross RA (1996) Kinetics and motility of the Eg5 microtubule motor. *Biochemistry* 35:2365–2373.
23. Kwok BH, et al. (2006) Allosteric inhibition of kinesin-5 modulates its processive directional motility. *Nat Chem Biol* 2:480–485.
24. Schaar BT, Chan GK, Maddox P, Salmon ED, Yen TJ (1997) CENP-E function at kinetochores is essential for chromosome alignment. *J Cell Biol* 139:1373–1382.
25. Wood KW, Sakowicz R, Goldstein LS, Cleveland DW (1997) CENP-E is a plus end-directed kinetochore motor required for metaphase chromosome alignment. *Cell* 91:357–366.
26. Espeut J, et al. (2008) Phosphorylation relieves autoinhibition of the kinetochore motor Cenp-E. *Mol Cell* 29:637–643.
27. Kim Y, Heuser JE, Waterman CM, Cleveland DW (2008) CENP-E combines a slow, processive motor and a flexible coiled coil to produce an essential motile kinetochore tether. *J Cell Biol* 181:411–419.
28. Yardimci H, van Duffelen M, Mao Y, Rosenfeld SS, Selvin PR (2008) The mitotic kinesin CENP-E is a processive transport motor. *Proc Natl Acad Sci USA* 105:6016–6021.
29. Yildiz A, Tomishige M, Gennerich A, Vale RD (2008) Intramolecular strain coordinates kinesin stepping behavior along microtubules. *Cell* 134:1030–1041.
30. Tomishige M, Klopfenstein DR, Vale RD (2002) Conversion of Unc104/KIF1A kinesin into a processive motor after dimerization. *Science* 297:2263–2267.
31. Lakamper S, et al. (2010) The effect of monastrol on the processive motility of a dimeric kinesin-5 head/kinesin-1 stalk chimera. *J Mol Biol* 399:1–8.
32. Sardar HS, Luczak VG, Lopez MM, Lister BC, Gilbert SP (2010) Mitotic kinesin CENP-E promotes microtubule plus-end elongation. *Curr Biol* 20:1648–1653.
33. Walshaw J, Woolfson DN (2001) Socket: A program for identifying and analysing coiled-coil motifs within protein structures. *J Mol Biol* 307:1427–1450.
34. Hwang W, Lang MJ, Karplus M (2008) Force generation in kinesin hinges on cover-neck bundle formation. *Structure* 16:62–71.
35. Khalil AS, et al. (2008) Kinesin's cover-neck bundle folds forward to generate force. *Proc Natl Acad Sci USA* 105:19247–19252.
36. Rice S, et al. (1999) A structural change in the kinesin motor protein that drives motility. *Nature* 402:778–784.
37. Vale RD, Milligan RA (2000) The way things move: Looking under the hood of molecular motor proteins. *Science* 288:88–95.
38. Case RB, Rice S, Hart CL, Ly B, Vale RD (2000) Role of the kinesin neck linker and catalytic core in microtubule-based motility. *Curr Biol* 10:157–160.
39. Kutys ML, Fricks J, Hancock WO (2010) Monte Carlo analysis of neck linker extension in kinesin molecular motors. *PLoS Comput Biol* 6:e1000980.
40. Muthukrishnan G, Zhang Y, Shastry S, Hancock WO (2009) The processivity of kinesin-2 motors suggests diminished front-head gating. *Curr Biol* 19:442–447.
41. Du Y, English CA, Ohi R (2010) The kinesin-8 Kif18A dampens microtubule plus-end dynamics. *Curr Biol* 20:374–380.